Defect Detection in Solar Photovoltaic Systems Using Unmanned Aerial Vehicles and Machine Learning

Althea Miquela, Dhiraj Bagul, and Ahmed Aziz Ezzat
Rutgers, The State University of New Jersey,
Piscataway, NJ, 08854, USA
am2639@scarletmail.rutgers.edu, dhiraj.bagul@rutgers.edu, aziz.ezzat@rutgers.edu

Abstract

The rapid growth of solar energy installations worldwide calls for innovative solutions to optimize the operations and maintenance (O&M) activities in solar energy farms, with the ultimate goal of enhancing the economic outlook of solar power. Recently, there has been a growing interest in exploring the merit of emerging technologies such as unmanned aerial vehicles (UAVs) and artificial intelligence (AI) in driving smart O&M decisions for solar photovoltaic (PV) systems. Towards this goal, this paper presents a UAV-enabled, AI-powered framework to automate solar energy asset monitoring and fault detection. First, an experimental testbed has been set up at the Energy Lab at Rutgers University – New Brunswick, wherein a UAV is flown over an operational PV system to collect real-time, high-resolution aerial images of the solar panels under various operational and weather conditions. Then, a deep-learning (DL)-based framework is proposed to extract relevant features from the processed UAV images, which are then combined with exogenous weather parameters, in order to make a decision on the health status of the solar panel under inspection. Our extensive experiments on two prevalent fault modes, namely snow accumulation and shading, suggest that our proposed approach can effectively identify the occurrence of such defects in solar panels, with up to 95.6% accuracy, while maintaining a sensible balance between false and missed alarms. Our framework serves as a testament to the merit of combining UAV-enabled data acquisition with emerging AI technologies in order to automate and optimize O&M activities and asset management in solar farms.

Keywords
Fault Detection, Machine Learning, Operations and Maintenance, Solar Energy, Unmanned Aerial Vehicles.

1. Introduction
The growing demand for clean energy has led to an increased adoption of solar photovoltaic (PV) systems worldwide. By the end of 2022, the global installed cumulative capacity of solar PV systems has reached 1,185 GW, of which 240 GW have been commissioned in 2022 alone—an increase of 37% relative to 2021 (International Energy Agency, 2023). With such rapid expansion in scale and sophistication, there is an imminent need for effective solutions and technologies that can lower the operations and maintenance (O&M) costs in solar energy farms, and ultimately enhance the economic outlook of solar power.

To achieve this vision, there has been a growing interest in exploring the merit of emerging technologies such as robotics, automation, and Internet of Things (IoT) devices in optimizing O&M operations. Equipped with advanced imaging capabilities, Unmanned Aerial Vehicles (UAVs), colloquially known as drones, can provide a cost-effective solution to the inspection and monitoring of solar PV installations. Drones offer unparalleled advantages for conducting aerial inspections, allowing for remote, rapid, and detailed assessments of solar PV systems. By leveraging UAVs, solar asset operators can reduce inspection time, improve their fault diagnostic analyses, and significantly reduce the required resources and costs associated with manual inspections. A recent BloombergNEF report suggests that UAVs can cut down solar project inspection costs to as low as $302/MW/year, compared to $1,590/MW/year for traditional or manual inspection (Bullard, 2018).

In parallel, artificial intelligence (AI) and machine learning (ML) have recently demonstrated remarkable potential in several environmental applications, including but not limited to the renewable energy sector (Rolnick et al., 2022). According to a recent report, AI/ML technologies are expected to contribute towards lowering global greenhouse gas emissions by as much as 4% by 2030, which is roughly equivalent to 2.4 Gigatons of CO_2 emissions (Herweijer et al., 2020). Examples of emerging applications where AI/ML can have an outsized impact in the renewable energy sector include fault diagnostics and prognostics (Zhao et al., 2014, Rao et al., 2019), smart and predictive maintenance (Papadopoulos et al., 2021 and 2022), production control and optimization (Papadopoulos, 2023), weather and energy forecasting (Ezzat, 2019, Ye et al., 2023), electric load prediction (Sajjad et al., 2020), among others.

Despite the promise, significant innovations are still needed to further optimize and tailor the application of those disruptive technologies, namely UAVs and AI/ML, to streamline the automated inspection and defect analysis of solar energy assets. To this end, the *goal of this work* is to develop, test, and demonstrate a UAV-enabled, AI-powered framework for effective fault detection in solar PV systems.

1.1 Objectives

To achieve the abovementioned goal, the objectives of this work are three-fold, spanning experimental, modeling, and testing tasks: (*O1*) *Experimental*: To set up an experimental testbed wherein a UAV is flown over an operational solar PV system to assemble a diverse database of high-resolution aerial images under various weather conditions and fault modes; *(O2) Model Development:* To propose a multi-modal, deep-learning-based approach which combines the UAV-collected images, with exogenous weather parameters, in order to effectively make a decision about the health status of the inspected solar assets; *(O3) Testing and Validation:* To extensively evaluate and benchmark the performance of the proposed framework in identifying a number of prevalent fault modes in PV systems using real-world data collected from the experimental testbed against a variety of data-driven fault detection benchmarks.

2. Literature Review

There is a growing literature on the application of UAV-based inspection for solar asset monitoring and fault detection. Few recent comprehensive review efforts have provided different perspectives on the recent advances and challenges in this topic, including for PV systems (De Olivera et al., 2022, Yahya et a., 2022), as well as for concentrated solar thermal systems (Milidonis et al., 2023).

Our survey of the related recent efforts suggests that the literature can be broadly categorized into two main clusters, primarily based on the fault detection methods employed to analyze the UAV-collected images. The first cluster relies on segmentation-based approaches using computer vision algorithms, image filtering methods, and statistical analyses of key image features in order to identify and further localize the defect patterns in solar modules (Aghaei et al., 2015, Addabbo et al., 2017, Li et al., 2017, Tsanakas et al., 2017, Liao and Lu, 2021).

The second cluster bears on the recent advances in image-based machine learning (ML) to directly learn the underlying patterns within the UAV-collected images (or processed versions thereof). The models therein typically rely on deep-learning (DL)-based architectures that can effectively extract features from the aerial images, which are then used to classify those images into various fault modes and/or health statuses (Li et al., 2018, Li et al., 2019, Pierdicca et al., 2020, Su et al., 2021, Venkatesh et al., 2022).

Combined, those studies demonstrate the potential of UAVs and AI methods for effective solar asset monitoring and fault detection. Solar PV systems are subject to numerous fault modes, several of which are potentially "identifiable" using aerial imagery such as cracks, snail trails, yellowing, hot spots, shading effects, and soiling, including dust, snow, grimes, bird droppings, among others (Djordjevic et al., 2014). This work in particular focuses on snow accumulation and shading effects, with the potential to be expanded to further fault modes. Those two fault modes are prevalent in solar PV systems. In specific, shading is often caused by nearby structures, local clouds, as well as nearby trees and plants, especially when located in agricultural lands in the context of the so-called agrivoltaics (Chaudhary and Chaturvedi, 2018). On the other hand, snow coverage and accumulation on solar modules commonly takes place in PV systems especially when installed in cold climates where the weather conditions allow for frequent snowfall (Øgaard et al., 2021). Both faults are known to largely impact the efficiency of solar panels, and hence, efforts contributing towards their early detection can be crucial in taking timely correction measures, slowing the degradation of solar energy assets, minimizing the associated power losses, and ultimately, lowering the overall O&M costs.

3. Methods

We introduce the proposed UAV-enabled, AI-powered framework for solar asset fault detection in the schematic diagram of Figure 1. The framework comprises the following key steps: *(S1)* Experimental setup and data collection; *(S2)* Data processing and augmentation; *(S3)* Machine learning and fault detection. The details of each step are outlined in Sections 3.1 through 3.3, respectively.

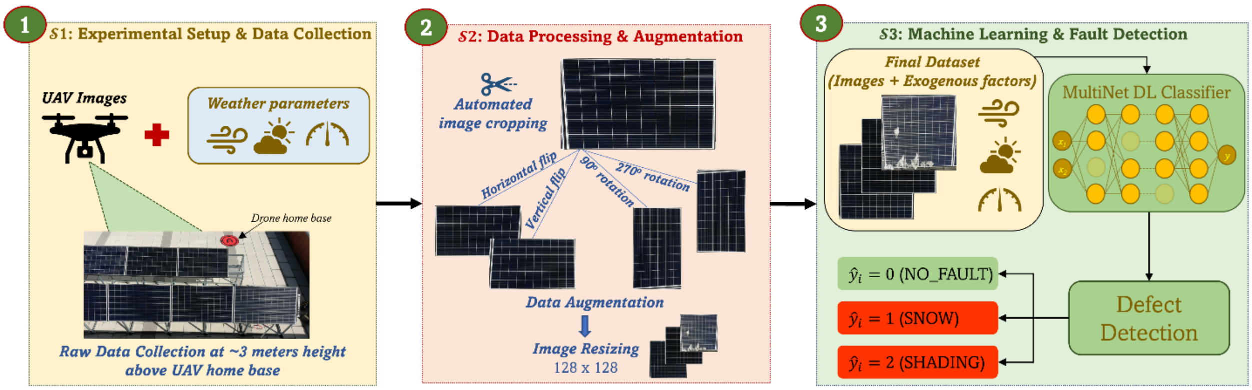

Figure 1: Overall workflow of our UAV-enabled, AI-powered fault detection framework for solar asset monitoring and diagnostics, starting from (S1) Experimental Setup & Data Collection; (S2) Data Processing & Augmentation; and (3) Machine Learning & Fault Detection.

3.1. Experimental Setup and Data Collection

The experimental testbed for this study is setup in the outdoor terrace of the Energy Laboratory located in Richard Weeks Hall of Engineering at Rutgers, The State University of NJ. The exact location of the Energy Lab is shown in Figure 2a. An off-grid 2.4 kW PV system, comprising eight operational solar panels have been fully operational at the laboratory since Summer 2021 and are used to power a number of indoor loads. Figure 2b shows an aerial view of the PV system under study. A research-grade Campbell Scientific meteorological station is located next to the solar system and includes the following sensors and components: (*i*) A wind monitor for measuring wind speed and direction, (*ii*) a digital thermopile pyranometer for measuring global horizontal irradiance (GHI), (*iii*) sensors to measure air temperature, relative humidity, and precipitation, and (*iv*) a CR6-Wi-Fi measurement and control datalogger, which is connected via Wi-Fi to a local PC which visualizes and stores the data in real-time.

In addition, an AUTEL Evo II Drone Explorer has been assembled with the required hardware and software components (See Figure 2c). The drone is equipped with a 48-megapixel Gimbal camera with 8K, 6K, DUAL Thermal payload options, and a 40-minute flight time, with obstacle avoidance features. Flight path planning and operation guidelines have then been carefully planned to ensure the data collection process by the research team is standardized and that the images were of the needed quality for downstream ML model training and development.

Figure 2: (a) Location of the Energy Lab at Rutgers University, New Brunswick; (b) Aerial view of the PV system under study; (c) The UAV assembled and used in this study (AUTEL Evo II Drone Explorer)

Data collection is performed using the UAV throughout the duration of the research project spanning from Fall 2022 to Spring 2023. In all experiments, the UAV is flown at about 3 meters high from the home base (shown in Figure 1b). To ensure a diverse dataset, the multiple flight conductions have been performed under different weather conditions, different months, and times of the day. The drone's camera has been configured to capture images in RGB mode. Once captured, the RGB images would be stored in JPEG format, together with other metadata (e.g., time of the day, GPS coordinates, color space) on a Secure Digital (SD) card, which is safely removed from the drone after the flight, and manually connected to the nearby lab server located indoors.

A total of 93 images have been collected across all UAV flights conducted. The raw images have an image size of 4000x3000 pixels^2 and are manually labelled into three health classes (or conditions). Letting y_i denote the true class of the ith image, then the three classes are listed as follows:

- NO_FAULT, indicating a healthy, fault-free solar panel, i.e., $y_i = 0$;
- SNOW, indicating snow presence on the inspected solar panel), i.e., $y_i = 1$;
- SHADING, indicating a partial shading on the inspected solar panel, i.e., $y_i = 2$.

In addition to the image data, the following weather parameters have been collected for each image: air temperature wind speed, and precipitation. Our exploratory analysis showed that those weather parameters have a decent predictive power in distinguishing the fault modes analyzed herein. Future research will look into the integration of additional weather and operational parameters.

3.2. Data Processing and Augmentation

The raw images are automatically segmented and cropped by removing the background and focusing entirely on the solar panel frame under inspection. Three sample cropped images corresponding to the three classes studied are shown in Figure 3. Note that the collected images for partial shading and snow accumulation may have different patterns than the samples shown in Figure 3. For example, the snow coverage in some panels may be mild (e.g., few snow spots on the panels) or severe (large patches or clusters of snow), or a combination thereof.

Figure 3: Samples of the Processed Images for (a) Healthy class (NO_FAULT); (b) Partial shading class (SHADING); and (c) Snow accumulation class (SNOW).

To perform image-based ML training (especially for deep-learning-based models), large and diverse datasets are needed. Thus, a data augmentation procedure has been implemented to over-sample the original raw image dataset, which we denote herein as $\mathcal{D}_{raw}$, by applying various flipping and rotational transformations. In specific, four transformations are applied: rotations of 90°and 270°, as well as horizontal and vertical flips. Those transformations have increased the raw image dataset $\mathcal{D}_{raw}$ by a factor of five, creating the augmented dataset, D_{aug}, which has a total of 465 images. Table 1 shows the number of samples per each fault mode, for both the raw and processed datasets, $\mathcal{D}_{raw}$ and D_{aug}, respectively. After augmentation, all images are then resized into square images of 128x128 pixels^2, which will be used for downstream ML model training and development, explained in detail in Section 3.2.

Table 1: Number of Images per class for the raw and augmented datasets, $\boldsymbol{\mathcal{D}_{raw}}$ and $\boldsymbol{\mathcal{D}_{aug}}$, respectively.

Fault Class	Raw Dataset, $\boldsymbol{\mathcal{D}_{raw}}$	Augmented Dataset, $\boldsymbol{\mathcal{D}_{aug}}$	Fraction
NO_FAULT	33	165	35.5%
SNOW	40	200	43.0%
SHADING	20	100	21.5%
Total	93	465	100%

3.2. Machine Learning and Fault Detection: A MultiNet Deep Learning Model

A MultiNet deep learning (DL) model is proposed for UAV-enabled fault detection in solar PV systems. The model architecture, shown in Figure 4, allows multi-modal learning by taking as input two streams of input data: (i) the augmented image data acquired using the Autel Evo II drone and processed using our data segmentation and augmentation procedure outlined in Section 3.1, and (*ii*) the exogenous weather data (namely, air temperature, precipitation, and wind speed). The output of the MultiNet model is a decision (i.e., a classification) about assigning each inspected solar panel into one of the three classes described in Table 1, namely: NO_FAULT, SNOW, and SHADING. Hereinafter, we denote the predicted class of the MultiNet model for the ith sample as $\hat{y}_i$.

As shown in Figure 4, the MultiNet model comprises a Convolutional Neural Network (CNN) for image-based feature extraction. CNNs are DL architectures that are tailored to effectively extract visual patterns directly from images and/or image-like inputs. Specifically, we implemented two feature blocks, each containing one CNN layer and one Max Pooling Layer. The CNN layer performs a convolution operation on previous layer outputs and extracts image features, and the Max Pooling Layer reduces the dimensionality of the data to maintain translational invariance. The output of the feature blocks is then fed to fully connected layers that learn the functional relation between the target class label and the key features of the UAV images. To incorporate the exogenous variables, we concatenate the image features from the final layer with the weather parameter values. Finally, we apply an activation on the final full-connected layer that combines image features and exogenous variables to obtain the final class predictions. This integration of image and weather data enables the model to leverage both visual information from the aerial images and external weather factors for more effective fault detection.

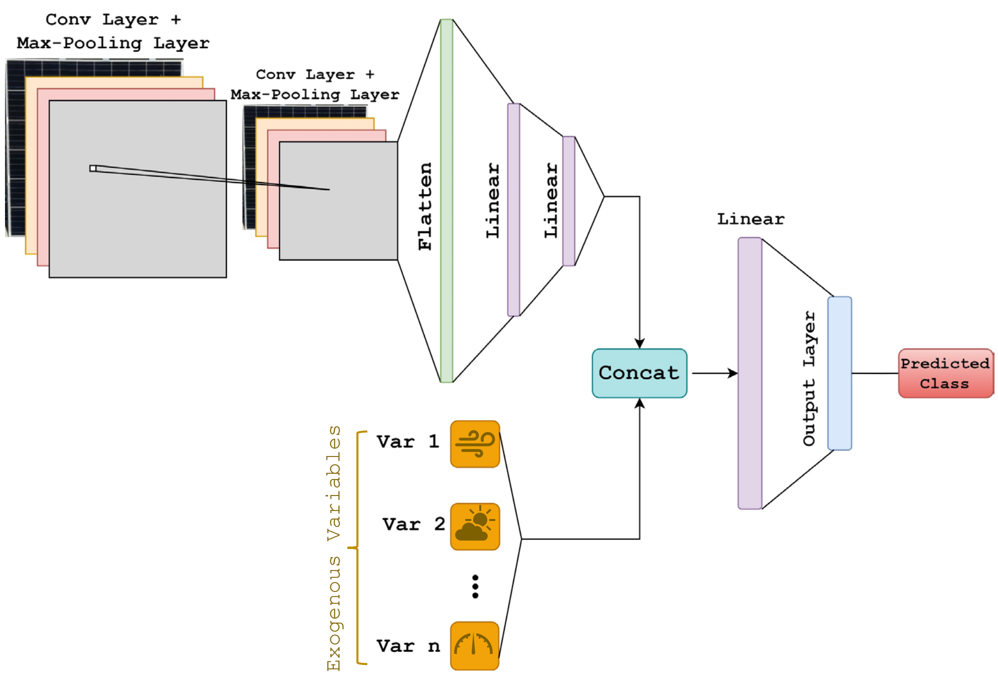

Figure 4: Proposed MultiNet architecture comprising of a CNN for image-based feature extraction, which is then integrated with exogenous weather parameters to output a final prediction for the solar panel under inspection

The proposed MultiNet model is implemented using PyTorch in Python. In specific, the MultiNet model is trained by minimizing the cross-entropy loss using the Adam optimizer, which combines the benefits of adaptive learning rates and momentum for improved training performance and convergence. A grid search was used to optimize the model hyperparameters including the learning rate, batch size, and number of epochs. The final parameters used in our model are: Batch size = 4, number of epochs = 500, and a learning rate of 0.001. This combination of hyperparameter values resulted in the best convergence performance.

4. Results and Discussion

4.1. Testing Procedure, Comparison Benchmarks, and Evaluation Metrics

For model evaluation and testing, the augmented dataset (along with the exogenous variables) has been divided into five randomized experiments, denoted hereinafter as $\mathcal{F}_1, \ldots, \mathcal{F}_5$. In each of the five experiments, 80% of the augmented dataset (~370 images) has been selected for training, with the remaining 20% being reserved for testing (~95 images). As seen in Table 1, classes are not equally represented. To avoid the negative impacts of class imbalance, the training sets for each experiment are stratified to down-sample over-represented classes and up-sample under-represented ones, thus avoiding severely dis-proportional class representations, while maintaining the 80/20 train-test split.

Two variants of our approach are implemented: MultiNet (*T*), which only includes temperature as the sole exogenous factor, and MultiNet (*T, WS, P*) which includes all three variables, namely, temperature, wind speed, and precipitation. In addition, we compare the performance of the MultiNet models against two data-driven benchmarks: (*i*) CNN: This is an image-based CNN model that only utilizes the processed image data as inputs, without the exogenous parameters; and (*ii*) Temp-Th: This is a simple, threshold-based procedure which classifies the images depending on whether the value of the air temperature for the testing sample exceeds the 95% percentile of the historical temperature values.

The four models (Temp-Th, CNN, and two variants of MultiNet) are compared using four different evaluation metrics: accuracy, precision, recall, and F-score. If we denote by $\boldsymbol{y_i}$ and $\boldsymbol{\hat{y}_i}$ the true and predicted class labels for the *i*th image, respectively, then accuracy is defined as $\frac{\sum_{i=1}^{n_{ts}} \mathbb{I}(y_i = \hat{y}_i)}{n_{ts}}$, where $\boldsymbol{n_{ts}}$ is the number of testing samples, while $\mathbb{I}(\cdot)$ is the indicator function. Precision is defined as $\frac{TP}{TP+FP}$, where $\boldsymbol{TP}$ and $\boldsymbol{FP}$ denote true and false positives, respectively. Recall, on the other hand, is defined as $\frac{TP}{TP+FN}$, where $\boldsymbol{FN}$ denotes false negatives. The F_1-score is the harmonic mean of the precision and recall, and is defined as $\frac{2 \times Precision \times Recall}{Precision + Recall}$.

4.2. Numerical Results and Discussion:

The evaluation metrics described in Section 4.1. are evaluated for each individual experiment, $\boldsymbol{\mathcal{F}_1, \ldots, \mathcal{F}_5}$, and then the average and standard deviation across the five experiments are calculated and reported in Table 2.

Table 2: Evaluation metrics for the four models considered herein, namely: Temp-Th, CNN, MultiNet (T), and MultiNet (T, WS, P). The numbers in parentheses denote the standard deviation across the five randomized experiments, $\boldsymbol{\mathcal{F}_1, \ldots, \mathcal{F}_5}$. Bold-faced values denote best performance.

Eval. Metric	Temp-Th (95th percentile)	CNN (Image-based)	MultiNet (*T*)	MultiNet (*T, WS, P*)
Accuracy	51.1% (3.83)	84.2% (5.14)	**95.6%** (1.91)	**95.6%** (1.11)
Precision	42.7% (3.03)	79.1% (4.45)	94.8% (3.30)	**94.9%** (2.11)
Recall	42.6% (2.85)	82.2% (5.50)	94.4% (2.91)	**94.7%** (2.08)
F_1-score	35.5% (2.94)	78.8% (5.77)	94.4% (2.84)	**94.5%** (1.55)

Looking at the results in Table 2, we can make a few key observations. First, it obvious that deep-learning-based approaches (namely CNN and the MultiNet variants) are much more effective than simple rule-based benchmarks. In specific, the CNN model achieves ~65% accuracy improvement over Temp-Th. Adding exogenous variables through the MultiNet models improves the performance by up to ~22% over CNN, and up to ~87% over Temp-Th. It also appears that both the univariate and multivariate versions of MultiNet perform similarly, with a slight advantage for the MultiNet (*T, WS, P*) relative to its univariate counterpart MultiNet (*T*). This advantage is demonstrated by the reduced standard deviation across all evaluation metrics, indicating a more robust/reliable classification performance, as well as in the slight boost in sensitivity (~0.3% increase) and F-score (~0.1% increase).

Those results convey two main findings. The first finding is concerning the merit of DL approaches relative to simple rule-based methods that are commonly used in practice for fault diagnostics and prognostics. The second finding is the additional benefit brought by the multi-modal learning of image data and exogenous weather factors within the DL models. While temperature is indeed a significant predictor of snow-related defects, fully leveraging its explanatory power is contingent on a well-designed ML framework (as in MultiNet), in contrast to simple rule-based benchmarks like Temp-Th. Furthermore, the inclusion of additional environmental factors, such as precipitation and wind speed, suggests that considering multiple environmental factors in conjunction with temperature can provide a marginal (but noticeable) increase in the accuracy and robustness of defect detection.

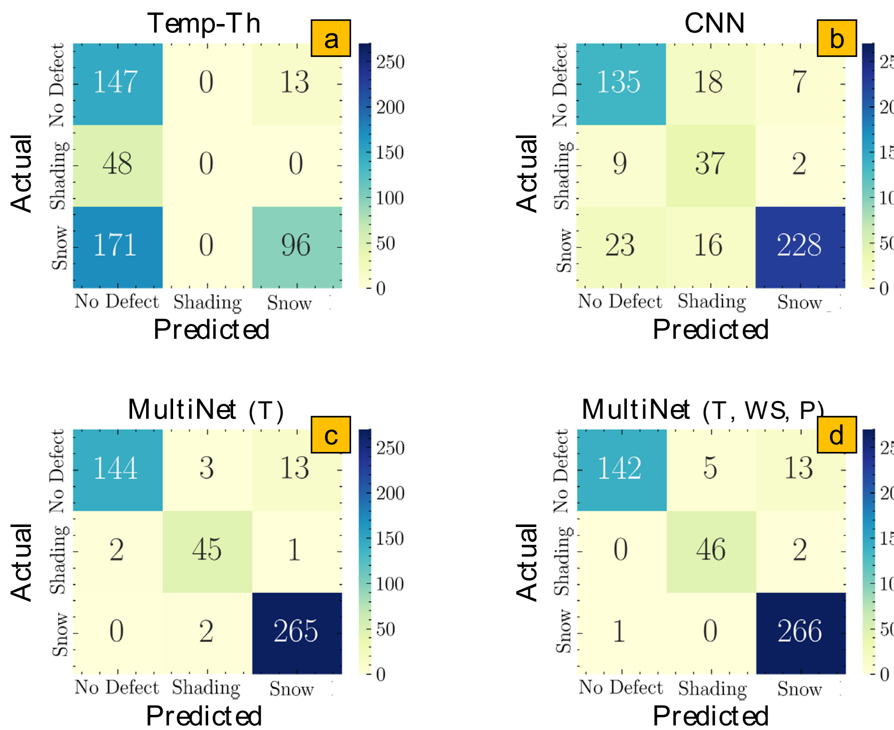

Figure 5: Confusion matrices for the four models considered herein, namely: Temp-Th, CNN, MultiNet (T), and MultiNet (T, WS, P).

The confusion matrices shown in Figure 5 are obtained by aggregating the results from all five experiments, and can further provide deeper insights about the fault diagnostic performance of the four competing models. In addition to confirming the findings conveyed from the analysis in Table 2, the confusion matrices in Figure 5 suggest that, for DL models, shading identification appears to be the easiest fault mode to detect across the three considered classes, with accuracies per class reaching up to 99.6% for MultiNet (*T, WS, P*). Despite that, it appears that the DL models struggle more in terms of false positives than in false negatives – that is, the models are more likely to mis-classify healthy samples as defective than vice-versa (up to 13 false positives for the shading class, and 5 false positives for the snow class). We believe that those false positives can be further reduced had our models been trained on a more diverse training dataset. For example, snow on solar panels can exist in many forms such as powdery snow, wet snow, or patches. Shading patterns –attributed to different cloud cover effects and/or other shadowing objects—can also be largely diverse and complex. Despite those challenges, we still conclude that our approach renders an overall satisfactory performance, as evidenced by both the aggregated results in Table 2, as well as the confusion matrices in Figure 5. On average, our approach achieves up to 95.6% and 94.6% in accuracy and F_1-score, respectively. This is a testament to the merit of the proposed AI framework in effective fault diagnostics and solar asset monitoring.

5. Conclusion and Future Research

In this work, we have proposed a UAV-enabled, AI-powered framework to automate asset monitoring and fault detection in solar PV systems. An experimental testbed has been set up at the Energy Lab at Rutgers University in NJ, which enabled the collection of real-time, high-resolution images of the solar PV system under various fault modes, as well as data about the exogenous weather parameters that may exhibit decent predictive power in explaining the fault occurrences in solar PV systems. Tested on a large number of testing samples, our proposed deep-learning-based approach, has been shown to effectively pinpoint prevalent fault modes in solar modules, while maintaining a sensible balance between false and missed alarms. Our proposed framework serves as an exemplar of the successful integration of emerging technologies such as UAVs and AI in offering a promising avenue for optimizing O&M activities in solar energy farms, thereby contributing to the wider adoption of solar power as a clean energy source.

This work opens the door for several interesting questions and potential extensions. As a case in point, it would be worth it to consider both visual and thermal imaging modes for the UAV. Thermal images can provide richer information, especially in regard to localizing snow- and overheating-related defects. In terms of methodology, we would like to explore (and potentially hybridize) various image-based ML approaches, including those based on graph-theoretic methods (Ezzat et al., 2021) or more advanced DL architectures (Xie et al, 2017). Finally, extending the proposed approach to include a larger number of fault modes such as cracks, dust, snail trails, hot spots, among others, is currently under investigation by the research team.

Acknowledgment

Althea Miquela has been supported through The Research Experiences for Undergraduates (REU) program by the U.S. National Science Foundation (NSF Grant #: ECCS-2114422).

References

Addabbo, P., Angrisano, A., Bernardi, M.L., Gagliarde, G., Mennella, A., Nisi, M. and Ullo, S., A UAV infrared measurement approach for defect detection in photovoltaic plants, *Proceedings of the 2017 IEEE International Workshop on Metrology for AeroSpace (MetroAeroSpace)*, pp. 345-350, 2017.

Aghaei, M., Grimaccia, F., Gonano, C.A. and Leva, S., Innovative automated control system for PV fields inspection and remote control, *IEEE Transactions on Industrial Electronics*, 62(11), pp.7287-7296, 2015.

Bullard, N., Why Power Companies Love Drones, *BloombergNEF*, 2018, URL: https://about.bnef.com/blog/bullard-power-companies-love-drones/ (last accessed: May 2023).

De Oliveira, A.K.V., Aghaei, M. and Rüther, R., Automatic inspection of photovoltaic power plants using aerial infrared thermography: A review, *Energies*, 15(6), pp.2055, 2022.

Djordjevic, S., Parlevliet, D. and Jennings, P., Detectable faults on recently installed solar modules in Western Australia, *Renewable energy*, 67, pp.215-221, 2014.

Ezzat, A., Jun, M., and Ding, Y., Spatio-temporal short-term wind forecast: A calibrated regime-switching method, *The Annals of Applied Statistics*, 13(3), pp.1484, 2019.

Ezzat, A.A., Liu, S., Hochbaum, D.S. and Ding, Y., A graph-theoretic approach for spatial filtering and its impact on mixed-type spatial pattern recognition in wafer bin maps, *IEEE Transactions on Semiconductor Manufacturing*, 34(2), pp.194-206, 2021.

Herweijer, C., Combes, B. and Gillham, J., How AI Can Enable a Sustainable Future? Technical Report, 2020, URL: https://www.pwc.co.uk/sustainability-climate-change/assets/pdf/how-ai-can-enable-a-sustainable-future.pdf (Last accessed: May 2023).

International Energy Agency (IEA), PVPS Programme, Snapshot of Global PV Markets 2023, *Technical Report*, IEA-PVPS T1-44:2023, 2023, URL: https://iea-pvps.org/wp-content/uploads/2023/04/IEA_PVPS_Snapshot_2023.pdf (last accessed: May 2023).

Li, X., Yang, Q., Chen, Z., Luo, X. and Yan, W., Visible defects detection based on UAV-based inspection in large-scale photovoltaic systems, *IET Renewable Power Generation*, 11(10), pp.1234-1244, 2017.

Li, X., Yang, Q., Lou, Z. and Yan, W., 2018. Deep learning-based module defect analysis for large-scale photovoltaic farms, *IEEE Transactions on Energy Conversion*, 34(1), pp.520-529, 2018.

Li, X., Li, W., Yang, Q., Yan, W. and Zomaya, A.Y., An unmanned inspection system for multiple defects detection in photovoltaic plants, *IEEE Journal of Photovoltaics*, 10(2), pp.568-576, 2019.

Liao, K.C. and Lu, J.H., Using UAV to detect solar module fault conditions of a solar power farm with IR and visual image analysis, *Applied Sciences*, 11, no. 4, p.1835, 2021.

Milidonis, K., Eliades, A., Grigoriev, V. and Blanco, M.J., Unmanned Aerial Vehicles (UAVs) in the planning, operation and maintenance of concentrating solar thermal systems: A review. Solar Energy, 254, pp.182-194, 2023.

Øgaard, M.B., Aarseth, B.L., Skomedal, Å.F., Riise, H.N., Sartori, S. and Selj, J.H., Identifying snow in photovoltaic monitoring data for improved snow loss modeling and snow detection, *Solar Energy*, 223, pp.238-247, 2021.

Papadopoulos, P., Coit, D. W., and Aziz Ezzat, A., STOCHOS: Stochastic opportunistic maintenance scheduling for offshore wind farms, *IISE Transactions*, 1-15, 2022.

Papadopoulos, P., Coit, D. W., and Aziz Ezzat, A., Seizing opportunity: maintenance optimization in offshore wind farms considering accessibility, production, and crew dispatch, *IEEE Transactions on Sustainable Energy*, vol. 13, no. 1, pp. 111-121, 2021.

Papadopoulos, P., Fallahi, F., Yildirim, M., and Aziz Ezzat, A., Joint optimization of maintenance and production in offshore wind farms: Balancing the short-and long-term needs of wind energy operation, *arXiv Preprint,* arXiv:2303.06174, 2023.

Pierdicca, R., Paolanti, M., Felicetti, A., Piccinini, F. and Zingaretti, P., Automatic faults detection of photovoltaic farms: SolAIr, a deep learning-based system for thermal images. *Energies*, 13(24), p.6496, 2020.

Rao, S., Spanias, A. and Tepedelenlioglu, C., Solar array fault detection using neural networks, *Proceedings of the 2019 IEEE international conference on industrial cyber physical systems* (ICPS), pp. 196-200, 2019.

Rolnick, D., Donti, P.L., Kaack, L.H., Kochanski, K., Lacoste, A., Sankaran, K., Ross, A.S., Milojevic-Dupont, N., Jaques, N., Waldman-Brown, A. and Luccioni, A.S., Tackling climate change with machine learning, *ACM Computing Surveys (CSUR)*, 55(2), pp.1-96, 2022.

Sajjad, M., Khan, Z.A., Ullah, A., Hussain, T., Ullah, W., Lee, M.Y. and Baik, S.W., A novel CNN-GRU-based hybrid approach for short-term residential load forecasting. *IEEE Access,* vol. 8, pp.143759-143768, 2020.

Su, B., Chen, H., Liu, K. and Liu, W., RCAG-Net: Residual channel wise attention gate network for hot spot defect detection of photovoltaic farms, *IEEE Transactions on Instrumentation and Measurement*, 70, pp.1-14, 2021.

Chaudhary, A.S. and Chaturvedi, D.K., Analyzing defects of solar panels under natural atmospheric conditions with thermal image processing, *International Journal of Image, Graphics and Signal Processing*, 11(6), p.10, 2018.

Tsanakas, J.A., Ha, L.D. and Al Shakarchi, F., Advanced inspection of photovoltaic installations by aerial triangulation and terrestrial georeferencing of thermal/visual imagery, *Renewable Energy*, 102, pp.224-233, 2017.

Venkatesh, S.N. and Sugumaran, V., Machine vision-based fault diagnosis of photovoltaic modules using lazy learning approach. *Measurement*, 191, p.110786, 2022.

Xie, S., Girshick, R., Dollár, P., Tu, Z. and He, K., Aggregated residual transformations for deep neural networks, *Proceedings of the IEEE conference on computer vision and pattern recognition*, pp. 1492-1500, 2017.

Yahya, Z., Imane, S., Hicham, H., Ghassane, A. and Safia, E.B.I., Applied imagery pattern recognition for photovoltaic modules' inspection: A review on methods, challenges and future development, *Sustainable Energy Technologies and Assessments*, vol. 52, pp.102071, 2022.

Ye, F., Brodie, J., Miles, T. and Aziz Ezzat, A., AIRU-WRF: A Physics-Guided Spatio-Temporal Wind Forecasting Model and its Application to the US North Atlantic Offshore Wind Energy Areas, *ArXiv preprint arXiv:2303.02246*, 2023.

Zhao, Y., Ball, R., Mosesian, J., de Palma, J.F. and Lehman, B., Graph-based semi-supervised learning for fault detection and classification in solar photovoltaic arrays, *IEEE Transactions on Power Electronics*, vol. 30, no. 5., pp.2848-2858, 2014.

Biography

Althea Miquela received the B.Sc. degree in Industrial and Systems Engineering from Rutgers University, New Brunswick, NJ, USA in May 2023. She has worked as a research assistant with the Renewables and Industrial Analytics (RIA) Research Group under Prof. Aziz Ezzat where she has been supported through the NSF REU program. Her research interests include operations management and artificial intelligence, applied to renewable energy systems. Upon completion of her undergraduate studies, she will be working as a Systems Engineer at L3Harris Technologies.

Dhiraj Bagul completed his B.Tech. in Computer Engineering from the Savitribai Phule Pune University, Pune, India, followed by M.S. in Computer Science from Rutgers University, New Brunswick, NJ, USA, in May 2023. His research interests include Applied Machine Learning, Computer Vision, and Natural Language Processing.

Ahmed Aziz Ezzat is an Assistant Professor of Industrial & Systems Engineering at Rutgers University, NJ, where he leads the Renewables & Industrial Analytics (RIA) research group. Before joining Rutgers, Dr. Aziz Ezzat received his Ph.D. from Texas A&M University in 2019, and his B.Sc. degree from Alexandria, Egypt, in 2013, both in Industrial Engineering. His broad research interests are in the areas of data and decision sciences, forecasting analytics, machine learning, quality and reliability engineering, with focus on renewable energy analytics and industrial informatics. Dr. Aziz Ezzat is the recipient of the 2023 Best Track Paper Award from the IISE Energy Systems

Division (jointly with co-authors), the 2022 Data Analytics Teaching Award from the IISE DAIS Division, The 2020 IIF-SAS® research award from the Institute of International Forecasters and SAS corporation, the 2020 Rutgers OAT Teaching Award, and the 2014 IISE Sierleja Fellowship. He serves as the 2023-2024 president of the IISE Energy Systems (ES) Division and the secretary of the Forecasting for Social Good (F4SG) IIF cluster. His research has been supported by the National Science Foundation (NSF), The NJ Economic Development Authority, The Rutgers Energy Institute, as well as industry. He is an active member of INFORMS, IEEE-PES, and IISE.